Accepted Manuscript

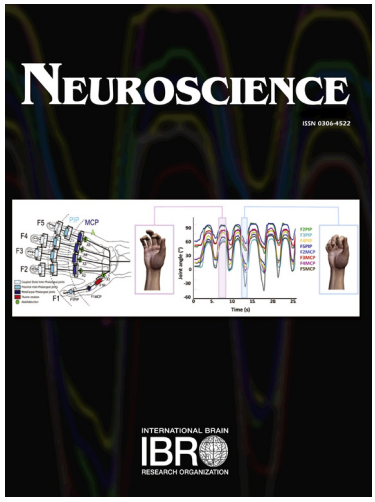

Research Article

Brain structural networks in mouse exposed to chronic maternal undernutrition

Jimena Barbeito-Andrés, Pablo M Gleiser, Valeria Bernal, Benedikt Hallgrímsson, Paula N Gonzalez

PII: S0306-4522(18)30249-5
DOI: https://doi.org/10.1016/j.neuroscience.2018.03.049
Reference: NSC 18387

To appear in: *Neuroscience*

Received Date: 18 March 2018
Accepted Date: 29 March 2018

Please cite this article as: J. Barbeito-Andrés, P.M. Gleiser, V. Bernal, B. Hallgrímsson, P.N. Gonzalez, Brain structural networks in mouse exposed to chronic maternal undernutrition, *Neuroscience* (2018), doi: https://doi.org/10.1016/j.neuroscience.2018.03.049

Brain structural networks in mouse exposed to chronic maternal undernutrition

Jimena Barbeito-Andrés[1,2*], Pablo M Gleiser[2], Valeria Bernal[3], Benedikt Hallgrímsson[4], Paula N Gonzalez[1]

1. ENyS - Unidad Ejecutora de Estudios en Neurociencias y Sistemas Complejos (UNAJ-CONICET-HNK). Av. Calchaquí 5402, Florencio Varela (1888), Buenos Aires, Argentina.

2. Grupo de Física Estadística e Interdisciplinaria (FiEstIn), Centro Atómico Bariloche. Av. Bustillo 9500, San Carlos de Bariloche (8400), Río Negro, Argentina.

3. CONICET, División Antropología, FCNyM, UNLP. 120 N1428, La Plata (1900), Buenos Aires, Argentina.

4. Department of Cell Biology and Anatomy, McCaig Institute for Bone and Joint Health, Alberta Children's Hospital Research Institute, University of Calgary. 3280 Hospital Drive NW, Calgary, Alberta, Canada T2N 4Z6.

*Correspondence to: Jimena Barbeito-Andrés, ENYS, Av. Calchaquí 5402, Florencio Varela (1888), Buenos Aires, Argentina, +54 (011) 4210-9000 (8011/8013), barbeitoj@gmail.com

Email addresses: Jimena Barbeito-Andrés: barbeitoj@gmail.com; Pablo M. Gleiser: gleiser@cab.cnea.gov.ar; Valeria Bernal: bernal.valeria@gmail.com; Benedikt Hallgrímsson: bhallgri@ucalgary.ca; Paula N. Gonzalez: paulan.gonza@gmail.com

ABBREVIATIONS

Co: Control diet

DTI: Diffusion tensor images

k: Nodal degree

L: Characteristic path length

MCP: Moderate calorie-protein restriction diet

Mean C: Mean clustering coefficient

MRI: Magnetic resonance images

PCA: Principal Component Analysis

PFA: Paraformaldehyde

R-C: Rich-club

ROI: Region of interest

SP: Severe protein restriction diet

SW: Small-worldness

ABSTRACT

Brain structural connectivity is known to be altered in cases of intrauterine growth restriction and premature birth, although the specific effect of maternal nutritional restriction, a common burden in human populations, has not been assessed yet. Here we analyze the effects of maternal undernutrition during pregnancy and lactation by establishing three experimental groups of female mice divided according to their diet: Control (Co), Moderate calorie-protein restriction (MCP) and Severe protein restriction (SP). Nutritionally restricted dams gained relatively less weight during pregnancy and the body weight of the offspring was also affected by maternal undernutrition, showing global growth restriction. We performed magnetic resonance images (MRI) on the offspring's brains after weaning and analyzed their connectivity patterns using complex graph theory. In general, changes observed in the MCP group were more subtle than in SP. Results indicated that brain structures were not homogeneously affected by early nutritional stress. In particular, the growth of central brain regions, such as the temporo-parietal cortex, and long integrative myelinated tracts were relatively preserved, while the frequency of short tracts was relatively reduced. We also found a differential effect on network parameters: network degree, clustering, characteristic path length and small-worldness remained mainly unchanged, while the rich-club index was lower in nutritionally restricted animals. Rich-club decrease reflects an impairment in the structure by which brain regions with large number of connections tend to be more densely linked among themselves. Overall, the findings presented here support the hypothesis that chronic nutritional stress produces long-term changes on brain structural connectivity.

KEYWORDS

Growth restriction; brain sparing; complex graphs; magnetic resonance imaging; rich-club

INTRODUCTION

The development of the central nervous system is a complex process that demands large amounts of energy as well as specific nutritional components (Morgane et al., 2002; Kuzawa et al., 2014; Barrickman, 2016). Since most of brain development occurs prenatally and during lactation, maternal nutrition has been identified as a key factor for brain growth and maturation both in human populations (Ivanovic et al., 2000; Odabaş et al., 2005; Kar et al., 2008) and in experimental animal models (Cordero et al., 1986; Morgane et al., 1993, 2002; Ranade et al., 2008, 2012; Antonow-Schlorke et al., 2011; Durán et al., 2011; Hunter et al., 2016). The experimental approaches have been mainly devoted to assess the effects of different conditions of maternal nutrient restriction on the brain of the offspring (Hunter et al., 2016). Different changes are found depending on the degree of restriction (from mild to severe deprivation), the developmental stage and the duration of the nutritional stress (there are studies in which the treatment is only induced in a part of the pregnancy, or throughout the whole gestation, or include lactation), the kind of nutrient that is reduced (e.g. protein restriction, calorie-protein restriction) as well as the animals used (most studies are done on rats although mice and non-human primates have also been used) (Alamy and Bengelloun, 2012). Overall, these works have mainly focused on histological and physiological alterations of specific brain regions while the effect of early malnutrition on the structural connectivity between them is still largely unknown. Understanding the consequences of environmental factors on the connectivity is particularly relevant given that it represents the anatomical support of information flow (Sporns et al., 2004).

In recent years, advances in methods for high resolution magnetic resonance imaging (MRI) have opened new possibilities for the assessment of structural properties of the whole brain. Among other advantages, MRI-based techniques provide the opportunity to track and visualize the myelinated tracts that link brain regions. The observed connections are commonly summarized as networks whose nodes and edges are formed by anatomical regions and tracts, respectively. Properties of such structural networks have been analyzed using complex graph theory, which allows inferences about connectivity patterns that are not possible from the study of elements in isolation (Sporns et al., 2005; Stam, 2014). The architectural properties of these networks were found to be strongly influenced by genetic, epigenetic and environmental factors (Hoff et al., 2013; Stam, 2014). Among them, special attention was paid to the probable effect of fetal growth restriction and preterm birth on structural connectivity (Ball et al., 2012; Batalle et al., 2012, 2014; Karolis et al., 2016). According to these works, the organization of brain structural connections is to some extent robust to perturbations in somatic growth, although they report changes in network properties. However, the causes of growth perturbation explored were the reduced placental flow, induced either by experimental ligation of uteroplacental vessels or by placental insufficiencies, and other maternal and fetal alterations rather than the maternal malnutrition per se, which is a common burden in several human populations. Other studies have used MRI to assess the effects of nutrition on human brain development (Isaacs, 2013; Vasu et al., 2014; Strømmen et al., 2015; Beauport et al., 2016), although the influence of other socio-environmental factors and comorbidities cannot be discarded (Hunter et al., 2016). A few experiments have done so in animal models (Sussman et al., 2013a, 2013b), which unlike human studies, can be used to isolate the influence of specific factors. However, none of previous experimental works has characterized the effect of early nutrient restriction on brain structural networks.

Here, we focus on maternal malnutrition as the source of growth restriction and explore its consequences in structural connectivity. As different kinds of nutrient restriction can produce variable effects on

phenotypic traits we applied two complementary designs. One experimental group that models the effect of maternal severe protein restriction while maintaining a constant supply of energy and other micronutrients, and another group that models the effect of moderate restriction in the total amount of food resulting not only in a protein reduction but in a global calorie-protein restriction. Since both kinds of nutrient restriction (severe protein and moderate calorie-protein) have different prevalence and affect different human groups worldwide (Latham et al., 1997; FAO, 2006), we used well-established experimental models to account for their effects on brain structural connectivity.

We previously demonstrated that chronic protein restriction affects maternal body weight and placental structure during early-middle pregnancy, and impairs body and brain growth of the offspring later during perinatal life (Gonzalez et al., 2016). Protein restriction applied only during pregnancy also produces several long-lasting physiological and behavioral changes on the offspring, including hyperinsulinemia and glucose intolerance, hyperleptinemia, diet-induced obesity, and changes in the anxiety profiles, sleep patterns and circadian rhythms (Barker et al., 1993; Sutton et al., 2010; Crossland et al., 2017). The effect of global reduction of the intake has been less explored, although some studies demonstrate that it also leads to modifications of the body weight (Smart et al., 1976; Zhang et al., 2010) and produces significant alterations on brain development, by affecting cell proliferation, cell death, myelinogenesis, neuronal process formation and cell motility, even when the reduction is moderate (Antonow- Schlorke et al., 2011). On the basis of these studies we hypothesize that chronic nutrient restriction during early life has important consequences in brain structural connectivity. If this were the case, we would also expect that altered connectivity relates to morphological changes on the anatomical elements that conform the network (brain regions and white matter tracts connecting them).

Here, maternal nutritional restriction was applied from early intrauterine life to the end of lactation because mouse newborns are relatively immature, and thus several developmental processes -such as increasing axonal and dendritic density and myelination- take place during postnatal life, while in humans and many other mammals part of these changes occur prenatally (Semple et al., 2013). It is worth noting that despite of such differences in the developmental timing between the mouse brain and other species, the sequence of key events in brain development is highly conserved (Clancy et al., 2001). Consequently, the temporal extension of the nutritional stress applied here leads to a wide coverage of key neurodevelopmental events.

In sum, through the combination of experimental models with mice, micro-MRI techniques and complex graph analyses, this study will contribute to discuss the extent in which connectivity properties are disrupted or maintained under the influence of a particular and controlled environmental factor.

EXPERIMENTAL PROCEDURES

Animals and experimental design

C57BL/6J male and female 4-week-old mice from the Animal Facility of Faculty of Veterinary, National University of La Plata, Argentina, were acclimatized during 4 weeks on a 12-h light 12-h dark cycle. After this period, nulliparous females were randomly divided into three groups: Control (Co), Moderate low calorie-protein (MCP) and Severe low-protein (SP), and they were mated overnight. During the mating period, two females of the same group were housed in a standard cage and, one hour before the beginning of the dark cycle, a male was introduced in the cage and it was left until the next morning at the beginning of the light cycle. At this moment, the male was removed from the cage and females were examined for postcoital vaginal plug as a signal of pregnancy confirmation. In those cases where postcoital plug was found, females were separated and housed in single cages. Dams from Co and SP groups received the corresponding diets starting from the day of pregnancy confirmation (E0) up to weaning of the pups. Co group had ad libitum access to a 20% protein diet with a caloric proportion of 3.8 Kcal/g (TD91352, Harlan Teklad, Madison) that is recommended for standard rodent breeding, while SP animals had ad libitum access to a protein-restricted diet (6%) in the form of casein and DL-Methionine but which has the same composition of calories as the Co diet (TD90016, Harlan Teklad, Madison). Moderate low calorie-protein (MCP) diet consisted on a reduction in the total amount of food dispensed to the dams. In this case, we followed the pair-feeding technique and from day E10, pregnant dams were fed with 80% of daily intake of a Co dam with similar weight and at the same day of pregnancy (Cesani et al., 2006). In order to obtain a better representation of each group and reduce potential bias due to maternal effects, analyzed animals derived from at least 3 dams in each group (n of dams: Co=6, MCP=3, SP=3).

All pups were weaned at day 20 of postnatal life (P20) and they were housed individually and fed standard diet until P34. Around this age, mice are experiencing adolescence stage characterized by the onset of their reproductive maturation and other physiological changes that preclude adulthood (Brust et al., 2015). Sample preparation consisted on deeply anesthetize P34 mice to be perfused with 4% paraformaldehyde (PFA) through the left ventricle to fix brain. After perfusion, extracranial tissues were removed and skulls were immersed into 4% of PFA during 48h and then they were stored in PBS until scanning. In total, 23 specimens were scanned and analyzed, including both males and females in similar proportions within each group (Co= 5 males and 5 females, MCP= 3 males and 3 females and SP= 3 males and 4 females). Body weights were compared between groups by means of ANOVA and using a post-hoc LSD test in order to distinguish multiple comparisons. Sexual dimorphism for morphometric measurements (body weight and brain volume) was evaluated by means of a Student's-t test.

All procedures were carried out according to the guidelines of the Canada Council on Animal Care and in compliance with the Committee for the Care and Use of Experimental Animals (CICUAL) of the Faculty of Veterinary of the National University of La Plata (Protocol number 42-2-14P). This study does not include any kind of human sample.

MRI acquisition and network construction

Fixed brains were scanned in a 9.4T animal MRI scanner (Bruker 9.4T BioSpec, Experimental Imaging Centre of the University of Calgary, Canada) to obtain high resolution MRI. T2-weighted echo-gradient

sequences, with TE 10 ms and field-of-view 15 x 15mm and matrix size of 128 x 128 x 30 were carried out. From these images, twenty-four regions of interest (ROIs) were manually segmented (Table 1) following Allen Reference Atlas available at http://www.brain-map.org/ Lein et al., (2007) and Dorr et al., (2008) and using Avizo software. From three-dimensional reconstructions, a volumetric estimation of each parcellated ROI was obtained.

Connections between previously parcellated ROIs were extracted by means of an algorithm that reconstructs tractography from diffusion tensor images (DTI) with 30 directions using software tools of MedInria (Toussaint et al., 2007) and DSI Studio (http://dsi-studio.labsolver.org/). By this procedure, we obtained a matrix containing the number of tracts that were reconstructed between each pair of nodes (i and j). Because the number of tracts is expected to be strongly associated with the volume of regions, we performed a standardization taking into account the volumes of the two participating nodes. Each edge was thus defined as $e_{ij} = \frac{VOL_i + VOL_j}{2n\ tracts}$, where VOL_i and VOL_j correspond to the volumes of the two connected nodes and n is the total number of tracts connecting them. These values were used to estimate a weighted connectivity matrix for each specimen that reflects its brain structural connections. Further data analysis is based on these weighted connectivity matrices.

Network analyses

Concepts and analyses based on graph theory were used to quantify patterns of brain connectivity. Here, brain networks were defined by their nodes (parcellated ROIs) and edges (given by the weights of the weighted connectivity matrix defined above) connecting pairs of nodes. All network measures were computed using Brain Connectivity Toolbox (Rubinov and Sporns, 2010) and the package igraph for R (Csardi and Nepusz, 2006).

First, a set of basic and general parameters were estimated to describe global aspects of networks and compare experimental groups. As a measure of network segregation, we used the clustering coefficient as defined by Onnela et al., (2005) for weighted matrices. This measure represents the intensity of edge triangles around a node and is defined as: $C_i = \frac{1}{s_i(k_i-1)} \sum_{j.k} \frac{(w_{ij}+w_{ik})}{2} a_{ij} a_{ik} a_{jk}$, where s_i corresponds to the strength of node *i*. According to this definition, only those link weights that were adjacent to node *i* sw_{ij} and w_{ik} are considered and a link between nodes *j* and *k* is required. The clustering coefficients of the 24 nodes were averaged to obtain the mean clustering coefficient (mean C) for each specimen. To describe the global network integration, we computed the characteristic path length (L) as the average of all the shortest paths connecting each node with all nodes, where the shortest path between two nodes is defined as the minimum sequence of nodes that links them. The formula used to obtain L was the following: $L = \frac{1}{n(n-1)} \sum_{i \neq j} d(v_i, v_j)$, where *n* is the number of nodes, and $d(v_i, v_j)$ refers to the shortest distance between nodes *i* and *j*.

Related to the previously described parameters, we estimated a measure of small-worldness (SW) for each specimen. A small-world pattern is defined by having a characteristic path length similar to a random equivalent network and a larger clustering coefficient (Watts and Strogatz, 1998). To assess whether the mouse brain networks studied here follow the small-world pattern, the network of each specimen was compared to a sample of one hundred random networks with the same degree and strength. In order to compare normalized values, we calculated the ratios between the original parameters for clustering (C_p) and characteristic path length

(L_p) and the same values for the random sample of networks (C_r and L_r). Finally, the SW value was obtained by dividing the normalized values of C and L, where $SW = \frac{C_p/C_r}{L_p/L_r}$. If SM values are larger than 1, then a small-world pattern can be designated.

In addition, we developed a complementary approach to assess global similarity between groups regarding their patterns of connectivity. The procedure consisted in estimating a median weighted connectivity matrix per group by obtaining the median value of each weight within the group. Then, each median weight value of the matrix of one group was regressed on the corresponding median weight of another group to account for their correlation and, therefore their similarity.

We also analyzed the influence of individual nodes. Nodal degree (k) was calculated by counting the number of edges connected to each node in all specimens. Then, frequency distributions for nodal degree were built separately for the three experimental groups. In addition, nodal efficiency was estimated on the neighborhood of each node as the inverse average shortest path connecting each node with the rest of them (Latora and Marchiori, 2001). Also, nodal betweenness centrality was computed as the portion of all shortest paths that include a given node. This measure reflects the participation of a node in the network. Finally, in order to obtain a more detailed description of the patterns of those regions that are central to the network, we analyzed the rich-club (R-C) structure. We followed Karolis et al., (2016) to construct a normalized R-C index to better compare groups. To this end, a raw R-C index was obtained as proposed by Opsahl et al., (2008) and multiplied it by the ratio of the number of nodes of the R-C and the total number of nodes in the network. After exploration, this normalized R-C index was calculated for a range of k-values from 6 to 19. Once values for each specimen were obtained, we calculated mean values and deviations by experimental group.

For those parameters where we found a remarkable dispersion of values, we performed a Bartlett test to assess the similarity of variances between groups. In this analysis two sets of values are compared to determine whether their variances could derive from the same population or they are as dissimilar as to be improbable.

Variation of spatial parameters: node size and tract length

In order to assess to what extent variation in the size of those elements that conform the nodes and links of the brain networks can impact on network topology, we analyzed the volume of the ROIs and the length of the tracts that connect them. First, a Principal Component Analysis (PCA) was carried out on ROIs volumes of the three samples to summarize the main axes of size variation. The aim of the PCA is to extract new axes that are linear combinations from the original variables (in our case, volumes of the ROIs). The output of PCA is then a set of orthogonal axes, where each one resumes variation of those traits that change in a coordinated fashion. The first PC resumes the maximum amount of variation and the other axes successively less variation. In addition, the loading of each original variable on each PC can be analyzed to have an estimation of the contribution of these particular variables to the new axes. For computing PCA, we used the function prcomp from R.

To better capture patterns of correlated variation in size among ROIs and inter-group differences in these patterns, we estimated partial correlation matrices for each group and plotted their values as heatmaps to detect the intensity and the direction of coordinated variation between regions in each group. Partial correlation was preferred in this case because it provides a measure of association between the size variation of two ROIs

while variation in other variables is controlled. These analyses were carried out using the R package ppcor (Kim et al., 2015).

Finally, the number of tracts connecting each pair of ROIs and the mean length of these sets of tracts were obtained from tractography. We analyzed the frequency distribution of these mean tract lengths as well as the total mean length per specimen. Inter-group comparisons were carried out by means of ANOVA and post-hoc LSD test.

RESULTS

Effects of nutrient restriction on weight and brain size

Weight changes in the dams along pregnancy as well as in the offspring reflected the metabolic effect of nutrient restriction in our study. At the pregnancy confirmation (E0.5), there were no significant differences between dams' body weight (mean values and standard deviations: Co=21.38g ±1.71, MCP=20.85g ±0.81, SP=21.31g ±1.5), while by the end of pregnancy (E18.5) comparisons indicated significant differences ($p<0.05$) between Co and both restricted groups (Co=37.65g ±1.71, MCP=34.38g ±3.12, SP=31.75g ±1.72). These differences became more evident when mothers' weight gain is evaluated: Co gained in average 76.82% of weight in the time between E0.5 and E18.5, while MCP increased the 64.64% and SP only gained 49.12%. In spite of this variation, we did not detect any case of premature birth and all specimens were born between E19.5 and E20.5.

Concerning the effect of the diet on the offspring, we evaluated body weight at P34, which corresponds to the moment when experimental treatments were completed. Here, significant differences ($p<0.01$) between Co and restricted groups were found (mean values and standard deviations: Co=17.61g ±2.87, MCP=14.18g ±1.78, SP=12.51g ±1.99). When sexual dimorphism was analyzed at P34 within each group, no significant differences were found in the body weight between sexes. At this age, brain volumes of Co (432.57mm^3 ±21.25) were highly significantly larger ($p<0.01$) than those from MCP (373.83mm^3 ±6.81) and SP (352.74 mm^3 ±14.87). No significant sexual dimorphism was detected within groups regarding brain volume.

Patterns of connectivity

Fig. 1 shows the results for global connectivity network parameters. Although groups largely overlapped, mean clustering (mean C) was slightly larger in SP than in Co group (Fig. 1a). It is also interesting to note that the dispersion of MCP, and to a lesser extent of SP, increased (Fig. 1a). In fact, a Barlett test for variance homogeneity showed that dispersion of the mean C parameter in MCP was significantly larger than in Co, while SP showed only a marginally significant difference with Co (Table 2). The characteristic path length (L) also showed a remarkable overlapping of groups with a larger dispersion in MCP and SP than Co (Fig. 1b), although only MCP showed a significantly increased variance (Table 2). In addition, small-worldness (SW) showed a subtle decrease in SP, but this difference was not significant and the coefficient of all specimens was larger than 1 suggesting a maintained small-worldness structure in all cases (Fig. 1c). Overall, main measures of global network segregation and integration showed that, although the parameters are largely conserved for all experimental groups, some subtle differences are observed between control and nutritional restricted groups (Fig. 1). In general, these results are in agreement with the pair-wise regressions of the median weighted connectivity matrices. We found a linear relationship among weights of connectivity matrices in all the between-group comparisons (Fig. 2). The correlation values between all pairs of groups were significant (Co vs MCP $r= 0.966$ $p<0.0001$; Co vs SP $r= 0.913$ $p<0.0001$; MCP vs SP: $r= 0.934$ $p<0.0001$), indicating that general network structure was preserved in both nutritionally restricted groups. It is worth noting that R-squared was the largest for the comparison between Co and MCP and the smallest for Co and SP (Fig. 2).

The frequency distributions of k for the three groups are shown in Fig. 3a. The curves are very similar, and present a slightly skewed shape, that overlaps in the whole k range for the three groups (Fig. 3a). For nodal centrality we did not find any differences among groups although a detailed analysis of the rich-club structure of

these nodes showed some differences. In all experimental groups, the rich-club (R-C) index increases smoothly for relatively small R-C degrees, and then grows steeply for those degrees larger than k= 14 that more probably correspond to hubs (Fig. 3b). R-C indices were systematically lower for SP, which is especially evident for R-C degrees larger than 15 (Fig. 3b). Regions and links that participate in the R-C for nodes with degree larger than 15 are showed per group (Fig. 3c). A striking result is that all experimental groups shared most of nodes involved in R-C relations: temporo-parietal cortex, striatum, hippocampus and midbrain. In the figures representing a transversal view of brains, it is evident that these regions are all centrally placed in relation to the antero-posterior axis of the brain (Fig. 3c). However, a difference was found for the SP group, in which the thalamus was not included into the regions that conformed R-C structures (Fig. 3c).

Properties of nodes and tracts

The first two PCs performed on ROIs volumes account for more than 75% of variation. PC1 is linearly related to total brain volume ($r=0.891$, $p<0.0001$) and the regions that contribute the most to the variation along this axis are the temporo-parietal cortex and the cerebellum (Fig. 4). All regions showed positive loadings on PC1, which reflects that this axis mostly summarizes absolute size differences. Along PC1, specimens belonging to Co group occupied more positive positions suggesting that their temporo-parietal cortex and cerebellum are relatively larger. On the other hand, SP specimens were placed towards the negative values of PC1, indicating an opposite pattern to Co, while MCP group occupied an intermediate position. The second PC (PC2) is less associated with total brain volume changes ($r=0.424$, $p=0.044$) and groups overlapped along this axis. PC2 loadings of ROIs showed a particular pattern where temporo-parietal cortex is negative while cerebellum is the most positive (Fig. 4). This means that PC2 captures some differences in relative size among specimens. In particular, a portion of size variation of temporo-parietal cortex is decoupled from variation of other important regions, especially the cerebellum (Fig. 4).

Partial correlation matrices showing the association between volumes of ROIs are displayed in Fig. 5 as heatmaps. The ordination of the regions is given by a hierarchical clustering algorithm. In Co group, we observed two well defined clusters, where correlations between regions of the same cluster are generally negative while inter-cluster correlations tend to be positive or very low. In both restriction groups this structure is relatively modified and those two big blocks are not as clear as in Co. In addition, the proportion of positive correlations is relatively reduced in MCP and SP (Fig. 5). Another result deriving from these heatmaps involves those regions that participate of R-C structures in previously described connectivity networks. In Co, most of the ROIs that were central in the connectivity networks, showed correlation values near to 0 between them. In other words, their sizes did not present correlated variation. On the other hand, for the restricted groups several R-C regions such as the temporoparietal cortex and the midbrain had negative or positive correlated variation with other central regions (Fig. 5).

The total number of tracts between all pairs of ROIs reconstructed in the tractography showed similar values and no significant differences between experimental groups in this tract property (mean values and standard deviations: Co=1513.10 ±41.67, MCP=1532.50 ±177.46, SP=1471.14 ±148.63). In contrast, significant differences between groups were found for tract length. Fig. 6a shows the total mean tract length per specimen. Specimens SP had in average mean tract lengths longer than the other groups (Fig. 6a). The ANOVA test revealed that mean tract lengths are significantly different ($F=4.344$, $p=0.027$) between Co and SP groups (LSD

test p=0.009) and between MCP and SP (LSD test p=0.005). Because values in Fig. 6a correspond to the means per specimen, the pattern found may result from two different scenarios, the higher tract length might result from the presence of a relatively larger amount of longer tracts in SP or from a relatively smaller proportion of short tracts. To address these alternatives, we analyzed the frequency distributions of tract lengths. In all cases the distributions present a sharp peak followed by a quick decay and a flat tail (Fig. 6b), revealing the presence of many connections between close neighbors and also some connections between distant nodes. These distributions were fit with a Gamma distribution following Kaiser et al, (2009). The parameters for the distributions values are the following: Co: a=5.67, b=0.46, c=0.935, r^2=0.98; MCP: a=5.67, b=0.48, c=1.006, r^2=0.99; SP: a=5.14, b=0.57, c=0.95, r^2=0.99. Note that the distributions for Co and MCP are indistinguishable, and there are differences with SP. In fact, a shift is observed in SP group where shorter lengths have a relatively smaller frequency (Fig. 6b). When absolute frequency of tracts of SP is subtracted to the Co frequency, it is more evident that there is a drop of tracts with length between 1 and 3 mm in SP group (Fig. 6b inset). This drop in the frequency of short tracts in SP group is followed by an increase of tracts of 3-4 mm, but this change is not as pronounced as the drop in shorter tracts (Fig. 6b inset). Thus, we infer that higher total mean tract lengths of SP resulted from a relatively reduction in the number of shorter paths in SP animals rather than an actual increase in length. Finally, in order to understand if this difference in tract length distributions derived from a change in tracts connecting particular nodes or whether it was a generalized pattern, we estimated the mean tract length by node (i.e. the average tract length of all the tracts that link a node with any other node). We found that for most nodes SP had a larger mean tract length than Co group (Table 3), suggesting that this pattern cannot be associated to a restricted set of brain structures, but it is a generalized change.

DISCUSSION

Phenotypic traits are variably influenced by nutritional stress (Nijhout, 2003; Gonzalez et al., 2011). We found that experimentally induced nutritional restriction during prenatal and early postnatal life is associated with some significant changes in brain connectivity. In particular, our results suggest that early nutrient restriction affected the connectivity of highly connected brain regions, which was described by the rich-club (R-C) index. Brain networks of animals that were exposed to early and chronic nutritional deprivation had lower values of R-C index. This shift can be understood as a reduction in the magnitude of those connections that relate highly connected nodes with similar also highly connected structures. Recently, the impact of developmental disruptions on brain R-C organization has been analyzed in a sample of adults that were preterm born (Karolis et al., 2016). In contrast to our findings, the cortical R-C structures were strengthened in preterm cases, probably as a consequence of preservation of those connections and nodes that are central in the network. Some differences related to the nature of the perturbation can account for these contrasting results. Preterm individuals experience an early interruption of intrauterine life and, although some maturational events are altered, rich-club architecture may exhibit postnatal "catch-up". This explanation is supported by other studies that found patterns compatible with compensatory processes in long-term myelination after intrauterine growth restriction (Tolcos et al., 2011; Illa et al., 2013). In this line Batalle et al., (2014), who used an animal model of utero-placental ligation to reproduce intrauterine growth restriction, found that even when some changes in network structure were observed, those regions that were hubs in specimens that had growth restriction correspond to the same central regions in control ones. In our model, regions that are part of R-C structures are largely conserved between experimental groups, although SP showed a difference regarding the participation of the thalamus, a key subcortical structure especially known by their interaction with cortical regions. Due to the complex integration with other structures, the thalamus is involved in important aspects of the sensory-motor and cognitive functions (Schmitt and Halassa, 2017). The fact that in SP the thalamus is not among the R-C structures does not necessarily imply that interactions with other regions are not guaranteed by direct or indirect ways. However, this shift may impact on the performance of those functional circuits where the thalamus is involved.

We also found remarkable differences in the total tract length along with a reduction of the number of short tracts in relation to longer tracts in animals under chronic nutrient restriction. Because brain networks are spatially defined, there are some constraints that do not depend on the topology itself but on the physical or spatial properties of nodes and links (Gastner and Newman, 2006; Bullmore and Sporns, 2012). Some structures of the network are more expensive to maintain than others. Several studies suggest that central and highly connected nodes are more demanding in blood flow and oxygen intake (van den Heuvel and Sporns, 2011; van den Heuvel et al., 2012; Alexander-Bloch et al., 2013b; Crossley et al., 2014). Also, long myelinated tracts that are usually less frequent in the brain and are mostly involved in integrative functions of the networks (van den Heuvel et al., 2012; Crossley et al., 2014), are more expensive to produce and their growth as well as the transmission of energy along them require more investment of the organism (Bullmore and Sporns, 2012). Therefore, prioritizing highly costly long myelinated tracts under metabolic and nutrient restriction may seem contradictory. On the other hand, perturbations of the integrative long-distance tracts may have several disrupting effects. In fact, different studies have showed that in severe neurological disorders, highly connected regions and long-distance edges are usually those that suffer more damage (Alstott et al., 2009; Achard et al.,

2012; Crossley et al., 2014). In other words, when costly central network elements are affected, brain functioning is compromised with cognitive or behavioral consequences. Accordingly, we hypothesize that long-distance integrative tracts were preferentially preserved at expenses of other local and probably redundant connections as a generalized response in the analyzed brain structures. This plastic response could allow maintenance of the integrity and topology of the network, reducing the impact of nutrient restriction in brain function. However, several studies have found alterations in behavior related to the exposure to maternal undernutrition (e.g. Villescas et al., 1981). Recently, studies using a similar protocol of maternal protein restriction to ours, described behavioral changes in the offspring such as an increase in anxiety, problems in social play, motivation, exploratory activity as well as disruptions of sleep (Belluscio et al., 2014; Crossland et al., 2017). More work is required to relate structural networks patterns to specific functional or behavioral outcomes.

Regarding morphological changes in the structures that conform the nodes of the networks, we found that the size of regions that are central to network structure are to some extent less affected. This is especially the case of the temporo-parietal cortex, which is relatively preserved compared to the global size reduction of the brain observed with nutrient restriction. Our results suggest that nutritional stress during development has a differential effect on size variation of analyzed regions. Consequently, the correlations among the sizes of brain regions were altered. Although these correlations between size of ROIs, measured by the thickness or volume, have been widely used to describe the structural covariation at a sample or population level, it is still an open question how they relate to functional and structural connectivity networks measured at the individual level (Alexander-Bloch et al., 2013b; Di et al., 2017). Some authors suggest a close relation under the assumption that the formation of axonal connections between regions is accompanied by structural covariation between them (Mechelli et al., 2005; Lerch et al., 2006). According to this reasoning, the early establishment of structural and functional connections between two regions would cause a trophic link that leads to coordinated maturation, which would be then expressed in coordinated variation of ROIs size (i.e. structural covariation) (Alexander-Bloch et al., 2013a, 2013b). However, there is also evidence supporting that structural covariance reflects information about a different kind of biological processes than white matter connectivity and metabolic or functional analyses (Gong et al., 2009; Di et al., 2017). Previous research on phenotypic variation have found that the observed patterns of association between morphological traits result from the tendency of the system to produce coordinated variation but correlations among traits are only evident when there is variation in the studied sample (Hallgrímsson et al., 2007; Hallgrímsson et al., 2009). In this study, we have shown that when size variation is introduced as a result of growth restriction, structural covariation changes substantially and this structure of covariation does not necessarily reflects the connectivity patterns of fibre tracts measured at the individual level.

Other basic network parameters such as degree distributions, clustering, characteristic path length and centrality of brain networks were maintained even when noticeable changes were found in the size of brain structures and other variables. One possibility is that these properties of connectivity networks were not sensitive to the induced stress. On the other hand, the observed pattern could be the result of buffering mechanisms unfolded during development to prevent seriously disrupting changes in brain network that could affect different brain functions as have been suggested in other cases (Baker et al., 2010). In this sense, plasticity of the nervous system during early life has been widely found to produce compensatory effects at different

anatomical levels (Blitz et al., 2004; Tovar-Moll et al., 2014). This possibility is partially supported by results provided by Batalle et al., (2014) and Karolis et al., (2016), which show that global integration of structural network is preserved at expenses of other features during growth perturbation.

Additionally, an increase in within-group variation was found for some connectivity parameters in the undernourished groups, despite the fact that mean values of network parameters remained unchanged. An increase in phenotypic variance has been associated with impaired buffering against environmental insults during development (Palmer 1994; Leung et al., 2000). Indeed, it has been found that a deprivation of nutritional resources in utero leads to an increase of dispersion in morphological (Gonzalez et al., 2014) as well as in behavioral traits (Eixarch et al., 2012). Our results can be indicative of perturbations of the developmental processes that produce those phenotypic traits. Further work on this topic, which includes larger samples, is required to reveal how nutritional stress impacts on the ability of the developing system to canalize brain growth.

In sum, our results indicated that chronic nutritional restriction had a differential influence on the properties of connectivity networks in mice brains. We modeled two scenarios of maternal nutritional restriction and showed that despite having a global impact on mothers and offspring's body weight as well as in brain volume, the effect on brain connectivity was heterogeneous with some variables more affected than others. Particularly, our results showed that the tendency for brain regions with large number of connections to be more densely linked among themselves was affected by early undernutrition. This was especially the case for the thalamus, although the functional consequences of such reduced connectivity need to be assessed. Concerning the components of connectivity networks, a remarkable finding was the relative preservation of the number of longer tracts after maternal severe protein restriction in comparison to local shorter connections. This last aspect (tract length) was one of the variables that remained unchanged for the moderate calorie-protein restriction case. In general, we found that both maternal nutritional stress models displayed different results, reinforcing the idea that more systematic studies comparing different protocols would be desirable to discern the specific effects of different environmental inputs on brain development. Overall, the findings presented here support the hypothesis that chronic nutritional stress produces long-term brain reorganization which is thought to underlie neurobehavioral changes, although the specific mechanisms responsible for the observed structural changes remains to be explored. In this sense, further studies are needed to assess whether the observed patterns result from a differential susceptibility intrinsic to brain elements or they are the consequence of compensatory mechanisms unfold in different ontogenetic stages.

ACKNOWLEDGES

We would like to acknowledge Dr. Jeffrey F. Dunn, David Rushforth and Tadeusz Foniok for their help with the MRI acquisitions (University of Calgary). We thank Raveena Dhaliwal for providing scripts for image processing (University of Calgary) and Dr. Fabian Nishida for his help with tissue fixation (Facultad de Ciencias Veterinarias, Universidad Nacional de La Plata). The experiments were conducted at the animal facility of the Faculty of Medicine in La Plata supervised by Dr. Laura Andrini, Dr. Marcela García and Dr. Ana Lía Errecalde (Cátedra de Citología, Histología y Embriología A, Universidad Nacional de La Plata). This study was supported by grants from Consejo Nacional de Investigaciones Científicas y Técnicas PIP 0603, Agencia de Promoción Científica y Tecnológica PICT 1810 2014/2017 and Universidad Nacional de La Plata N787 2015/2018.

AUTHOR CONTRIBUTIONS

Conceived and designed the experiments: JBA, VB, PNG. Performed the experiments: JBA, PNG. Analyzed the data: JBA, PMG, PNG. Wrote the paper: JBA, PMG, PNG. Critically revised the manuscript: VB, BH.

CONFLICTS OF INTEREST

None

REFERENCES

Achard S, Delon-Martin C, Vertes PE, Renard F, Schenck M, Schneider F, Heinrich C, Kremer S, Bullmore ET (2012) Hubs of brain functional networks are radically reorganized in comatose patients. Proc Natl Acad Sci 109:20608–20613.

Alamy M, Bengelloun WA (2012) Malnutrition and brain development: An analysis of the effects of inadequate diet during different stages of life in rat. Neurosci Biobehav Rev 36:1463-1480.

Alexander-Bloch A, Raznahan A, Bullmore E, Giedd J (2013a) The convergence of maturational change and structural covariance in human cortical networks. J Neurosci 33:2889–2899.

Alexander-Bloch A, Giedd JN, Bullmore E (2013b) Imaging structural co-variance between human brain regions. Nat Rev Neurosci 14:322–336.

Alstott J, Breakspear M, Hagmann P, Cammoun L, Sporns O (2009) Modeling the impact of lesions in the human brain Friston KJ, ed. PLoS Comput Biol 5:e1000408.

Antonow-Schlorke I, Schwab M, Cox L, Li C, Stuchlik K, Witte OW, Nathanielsz PW, McDonald TJ (2011) Vulnerability of the fetal primate brain to moderate reduction in maternal global nutrient availability. Proc Natl Acad Sci U S A 108:3011–3016.

Baker J, Workman M, Bedrick E, Frey MA, Hurtado M, Pearson O (2010) Brains versus brawn: An empirical test of barkers brain sparing model. Am J Hum Biol 22:206–215.

Ball G, Boardman JP, Rueckert D, Aljabar P, Arichi T, Merchant N, Gousias IS, Edwards AD, Counsell SJ (2012) The effect of preterm birth on thalamic and cortical development. Cereb Cortex 22:1016–1024.

Barker DJ, Gluckman PD, Godfrey KM, Harding JE, Owens JA, Robinson JS (1993) Fetal nutrition and cardiovascular disease in adult life. Lancet 341:938-941.

Barrickman NL (2016) The ontogeny of encephalization: tradeoffs between brain growth, somatic growth, and life history in Hominoids and Platyrrhines. Evol Biol 43:81–95.

Batalle D, Eixarch E, Figueras F, Muñoz-Moreno E, Bargallo N, Illa M, Acosta-Rojas R, Amat-Roldan I, Gratacos E (2012) Altered small-world topology of structural brain networks in infants with intrauterine growth restriction and its association with later neurodevelopmental outcome. Neuroimage 60:1352–1366.

Batalle D, Munoz-Moreno E, Arbat-Plana a, Illa M, Figueras F, Eixarch E, Gratacos E (2014) Long-term reorganization of structural brain networks in a rabbit model of intrauterine growth restriction. Neuroimage 100:24–38.

Beauport L, Schneider J, Faouzi M, Hagmann P, Hüppi PS, Tolsa J-F, Truttmann AC, Fischer Fumeaux CJ (2016) Impact of early nutritional intake on preterm brain: a magnetic resonance imaging study. J Pediatr 181:29-36.

Belluscio LM, Berardino BG, Ferroni NM, Ceruti JM, Cánepa ET (2014) Early protein malnutrition negatively impacts physical growth and neurological reflexes and evokes anxiety and depressive-like behaviors. Physiol Behav 129:237–254.

Blitz DM, Foster KA, Regehr WG (2004) Short-term synaptic plasticity: a comparison of two synapses. Nat Rev Neurosci 5:630–640.

Brust V, Schindler PM, Lewejohann L (2015) Lifetime development of behavioural phenotype in the house mouse (*Mus musculus*). Front Zool 12(Suppl 1):S17.

Bullmore E, Sporns O (2012) The economy of brain network organization. Nat Rev Neurosci 13:336–349.

Cesani MF, Orden AB, Oyhenart EE, Zucchi M, Muñe MC, Pucciarelli HM (2006) Growth of functional cranial components in rats submitted to intergenerational undernutrition. J Anat 209:137–147.

Clancy B, Darlington RB, Finlay BL (2001) Translating developmental time across mammalian species. Neuroscience 105:7–17.

Cordero ME, Trejo M, García E, Barros T, Rojas AM, Colombo M (1986) Dendritic development in the neocortex of adult rats following a maintained prenatal and/or early postnatal life undernutrition. Early Hum Dev 14:245–258.

Crossland RF, Balasa A, Ramakrishnan R, Mahadevan SK, Fiorotto ML, van den Veyver IB (2017) Chronic maternal low-protein diet in mice affects anxiety, night-time energy expenditure and sleep patterns, but not circadian rhythm in male offspring. PLoS One 12:e0170127.

Crossley NA, Mechelli A, Scott J, Carletti F, Fox PT, Mcguire P, Bullmore ET (2014) The hubs of the human connectome are generally implicated in the anatomy of brain disorders. Brain 137:2382–2395.

Csardi G, Nepusz T (2006) The igraph software package for complex network research. InterJournal:1695.

Di X, Gohel S, Thielcke A, Wehrl HF, Biswal BB (2017) Do all roads lead to Rome? A comparison of brain networks derived from inter-subject volumetric and metabolic covariance and moment-to-moment hemodynamic correlations in old individuals. Brain Struct Funct 222:3833-3845.

Dorr AE, Lerch JP, Spring S, Kabani N, Henkelman RM (2008) High resolution three-dimensional brain atlas using an average magnetic resonance image of 40 adult C57Bl/6J mice. Neuroimage 42:60–69.

Durán P, Miranda-Anaya M, Romero-Sánchez MDJ, Mondragón-Soto K, Granados-Rojas L, Cintra L (2011) Time-place learning is altered by perinatal low-protein malnutrition in the adult rat. Nutr Neurosci 14:145–150.

Eixarch E, Batalle D, Illa M, Muñoz-Moreno E, Arbat-Plana A, Amat-Roldan I, Figueras F, Gratacós E (2012) Neonatal neurobehavior and diffusion MRI changes in brain reorganization due to intrauterine growth restriction in a rabbit model. PLoS One 7:e31497.

FAO Food and Agriculture Organization of the United Nations (2006). The state of food insecurity in the world. Food and Agriculture Organization of the United Nations, Rome.

Gastner MT, Newman MEJ (2006) Optimal design of spatial distribution networks. Phys Rev E 74:016117.

Gong G, He Y, Concha L, Lebel C, Gross DW, Evans AC, Beaulieu C (2009) Mapping anatomical connectivity patterns of human cerebral cortex using in vivo diffusion tensor imaging tractography. Cereb Cortex 19:524–536.

Gonzalez PN, Hallgrímsson B, Oyhenart EE (2011) Developmental plasticity in covariance structure of the skull: effects of prenatal stress. J Anat 218:243–257.

Gonzalez PN, Lotto FP, Hallgrímsson B (2014) Canalization and developmental instability of the fetal skull in a mouse model of maternal nutritional stress. Am J Phys Anthropol 154:544–553.

Gonzalez PN, Gasperowicz M, Barbeito-Andrés J, Klenin N, Cross JC, Hallgrímsson B (2016) Chronic protein restriction in mice impacts placental function and maternal body weight before fetal growth. PLoS ONE 11(3): e0152227.

Hallgrímsson B, Jamniczky H, Young NM, Rolian C, Parsons TE, Boughner JC, Marcucio RS (2009) Deciphering the palimpsest: studying the relationship between morphological integration and phenotypic covariation. Evol Biol 36:355–376.

Hallgrímsson B, Lieberman DE, Young NM, Parsons T, Wat S (2007) Evolution of covariance in the mammalian skull. Novartis Found Symp 284:164–185; discussion 185–190.

Hoff GEA-J, van den Heuvel MP, Benders MJNL, Kersbergen KJ, De Vries LS (2013) On development of functional brain connectivity in the young brain. Front Hum Neurosci 7.

Hunter DS, Hazel SJ, Kind KL, Owens JA, Pitcher JB, Gatford KL (2016) Programming the brain: common outcomes and gaps in knowledge from animal studies of IUGR. Physiol Behav 164:233–248.

Illa M, Eixarch E, Batalle D, Arbat-Plana A, Muñoz-Moreno E, Figueras F, Gratacos E (2013) Long-term functional outcomes and correlation with regional brain connectivity by MRI diffusion tractography metrics in a near-term rabbit model of intrauterine growth restriction Frasch MG, ed. PLoS One 8:e76453.

Isaacs EB (2013) Neuroimaging, a new tool for investigating the effects of early diet on cognitive and brain development. Front Hum Neurosci 7:445.

Ivanovic DM, Leiva BP, Perez HT, Inzunza NB, Almagià AF, Toro TD, Urrutia MSC, Cervilla JO, Bosch EO (2000) Long-term effects of severe undernutrition during the first year of life on brain development and learning in Chilean high-school graduates. Nutrition 16:1056–1063.

Kaiser M, Hilgetag CC, van Ooyen A (2009) A simple rule for axon outgrowth and synaptic competition generates realistic connection lengths and filling fractions. Cereb Cortex 9:3001-3010.

Kar BR, Rao SL, Chandramouli BA (2008) Cognitive development in children with chronic protein energy malnutrition. Behav Brain Funct 4:31.

Karolis VR, Froudist-Walsh S, Brittain PJ, Kroll J, Ball G, Edwards AD, Dell'Acqua F, Williams SC, Murray RM, Nosarti C (2016) Reinforcement of the brain's rich-club architecture following early neurodevelopmental disruption caused by very preterm birth. Cereb Cortex 26:1322–1335.

Kim S (2015) ppcor: An R Package for a Fast Calculation to Semi-partial Correlation Coefficients. Communications for Statistical Applications and Methods 22: 665-674.

Kuzawa CW, Chugani HT, Grossman LI, Lipovich L, Muzik O, Hof PR, Wildman DE, Sherwood CC, Leonard WR, Lange N (2014) Metabolic costs and evolutionary implications of human brain development. Proc Natl Acad Sci U S A 111:13010–13015.

Latham MC (1997) Human nutrition in the developing world. Food and Nutrition Series - No. 29. FAO, Rome.

Latora V, Marchiori M (2001) Efficient behavior of small-world networks. Phys Rev Lett 87:198701.

Lein ES, Hawrylycz MJ, Ao N, Ayres M, Bensinger A, Bernard A, Boe AF, Boguski MS, Brockway KS, Byrnes EJ, Chen L, Chen L, Chen TM, Chin MC, Chong J, Crook BE, Czaplinska A, Dang CN, Datta S, Dee NR, Desaki AL, Desta T, Diep E, Dolbeare TA, Donelan MJ, Dong HW, Dougherty JG, Duncan BJ, Ebbert AJ, Eichele G, Estin LK, Faber C, Facer BA, Fields R, Fischer SR, Fliss TP, Frensley C, Gates SN, Glattfelder KJ, Halverson KR, Hart MR, Hohmann JG, Howell MP, Jeung DP, Johnson RA, Karr PT, Kawal R, Kidney JM, Knapik RH, Kuan CL, Lake JH, Laramee AR, Larsen KD, Lau C, Lemon TA, Liang AJ, Liu Y, Luong LT, Michaels J, Morgan JJ, Morgan RJ, Mortrud MT, Mosqueda NF, Ng LL, Ng R, Orta GJ, Overly CC, Pak TH, Parry SE, Pathak SD, Pearson OC, Puchalski RB, Riley ZL, Rockett HR, Rowland SA, Royall JJ, Ruiz MJ, Sarno NR, Schaffnit K, Shapovalova NV, Sivisay T, Slaughterbeck CR, Smith SC, Smith KA, Smith BI, Sodt AJ, Stewart NN, Stumpf KR, Sunkin SM, Sutram M, Tam A, Teemer CD, Thaller C, Thompson CL, Varnam LR, Visel A, Whitlock RM, Wohnoutka PE, Wolkey CK, Wong VY, Wood M, Yaylaoglu MB, Young RC,

Youngstrom BL, Yuan XF, Zhang B, Zwingman TA, Jones AR. (2007) Genome-wide atlas of gene expression in the adult mouse brain. Nature 445:168–176.

Lerch JP, Worsley K, Shaw WP, Greenstein DK, Lenroot RK, Giedd J, Evans AC (2006) Mapping anatomical correlations across cerebral cortex (MACACC) using cortical thickness from MRI. Neuroimage 31:993–1003.

Leung B, Forbes MR, Houle D (2000) Fluctuating asymmetry as a bioindicator of stress: comparing efficacy of analyses involving multiple traits. Am Nat 155:101–115.

Mechelli A, Friston KJ, Frackowiak RS, Price CJ (2005) Structural covariance in the human cortex. J Neurosci 25:8303–8310.

Morgane PJ, Austin-LaFrance R, Bronzino J, Tonkiss J, Díaz-Cintra S, Cintra L, Kemper T, Galler JR (1993) Prenatal malnutrition and development of the brain. Neurosci Biobehav Rev 17:91–128.

Morgane PJ, Mokler DJ, Galler JR (2002) Effects of prenatal protein malnutrition on the hippocampal formation. Neurosci Biobehav Rev 26:471–483.

Nijhout HF (2003) The control of growth. Development 130:5863–5867.

Odabaş D, Caksen H, Sar S, Unal O, Tuncer O, Ataş B, Yilmaz C (2005) Cranial MRI findings in children with protein energy malnutrition. Int J Neurosci 115:829–837.

Onnela J-P, Saramäki J, Kertész J, Kaski K (2005) Intensity and coherence of motifs in weighted complex networks. Phys Rev E 71:065103.

Opsahl T, Colizza V, Panzarasa P, Ramasco JJ (2008) Prominence and control: the weighted rich-club effect. Phys Rev Lett 101:1–4.

Palmer AR (1994). Fluctuating asymmetry analyses: a primer. In Markow TA (ed) Developmental instability: its origins and evolutionary implications. Kluwer Academic Publishers, Dordrecht, pp 355–364.

Ranade SC, Rose A, Rao M, Gallego J, Gressens P, Mani S (2008) Different types of nutritional deficiencies affect different domains of spatial memory function checked in a radial arm maze. Neuroscience 152:859–866.

Ranade SC, Sarfaraz Nawaz M, Kumar Rambtla P, Rose AJ, Gressens P, Mani S (2012) Early protein malnutrition disrupts cerebellar development and impairs motor coordination. Br J Nutr 107:1167–1175.

Rubinov M, Sporns O (2010) Complex network measures of brain connectivity : Uses and interpretations. Neuroimage 52:1059–1069.

Schmitt LI, Halassa MM (2017) Interrogating the mouse thalamus to correct human neurodevelopmental disorders. Mol Psychiatry 22:183–191.

Semple BD, Blomgren K, Gimlin K, Ferriero DM, Noble-Haeusslein LJ (2013) Brain development in rodents and humans: Identifying benchmarks of maturation and vulnerability to injury across species. Prog Neurobiol 106-107:1–16.

Smart JL, Tricklebank MD, Adlard BPF, Dobbing J (1976) Nutritionally small-for-dates rats: their subsequent growth, regional brain 5-hydroxytryptamine turnover, and behavior. Pediatr Res 10:807-811.

Sporns O, Chialvo DR, Kaiser M, Hilgetag CC (2004) Organization, development and function of complex brain networks. Trends Cogn Sci 8:418–425.

Sporns O, Tononi G, Kötter R (2005) The human connectome: A structural description of the human brain. PLoS Comput Biol 1:e42.

Stam CJ (2014) Modern network science of neurological disorders. Nat Publ Gr:1–13.

Strømmen K, Blakstad EW, Moltu SJ, Almaas AN, Westerberg AC, Amlien IK, Rønnestad AE, Nakstad B, Drevon CA, Bjørnerud A, Courivaud F, Hol PK, Veierød MB, Fjell AM, Walhovd KB, Iversen PO (2015) Enhanced nutrient supply to very low birth weight infants is associated with improved white matter maturation and head growth. Neonatology 107:68–75.

Sutton GM, Perez-Tilve D, Nogueiras R, Fang J, Kim JK, Cone RD, Gimble JM, Tschöp MH, Butler AA (2008) The melanocortin-3 receptor is required for entrainment to meal intake. J Neurosci 28:12946-12955.

Sussman D, Ellegood J, Henkelman M (2013a) A gestational ketogenic diet alters maternal metabolic status as well as offspring physiological growth and brain structure in the neonatal mouse. BMC Pregnancy Childbirth 13:198.

Sussman D, van Eede M, Wong MD, Adamson SL, Henkelman M (2013b) Effects of a ketogenic diet during pregnancy on embryonic growth in the mouse. BMC Pregnancy Childbirth 13:109.

Tolcos M, Bateman E, O'Dowd R, Markwick R, Vrijsen K, Rehn A, Rees S (2011) Intrauterine growth restriction affects the maturation of myelin. Exp Neurol 232:53–65.

Tonkiss J, Galler JR (1990) Prenatal protein malnutrition and working memory performance in adult rats. Behav Brain Res 40:95–107.

Toussaint N, Souplet JC, Fillard P (2007) MedINRIA: medical image navigation and research tool by INRIA. Proc. of MICCAI 7: 87.

Tovar-Moll F, Monteiro M, Andrade J, Bramati IE, Vianna-Barbosa R, Marins T, Rodrigues E, Dantas N, Behrens TEJ, de Oliveira-Souza R, Moll J, Lent R (2014) Structural and functional brain rewiring clarifies preserved interhemispheric transfer in humans born without the corpus callosum. Proc Natl Acad Sci 111:7843–7848.

van den Heuvel MP, Kahn RS, Goñi J, Sporns O, van den Heuvel MP (2012) Brain communication. Proc Natl Acad Sci U S A 109:11372–11377.

van den Heuvel MP, Sporns O (2011) Rich-club organization of the human connectome. J Neurosci 31:15775–15786.

Vasu V, Durighel G, Thomas L, Malamateniou C, Bell JD, Rutherford MA, Modi N (2014) Preterm nutritional intake and MRI phenotype at term age: a prospective observational study. BMJ Open 4:e005390.

Villescas R, Van Marthens E, Hammer RP (1981) Prenatal undernutrition: effects on behavior, brain chemistry and neuroanatomy in rats. Pharmacol Biochem Behav 14:455–462.

Watts DJ, Strogatz SH (1998) Collective dynamics of "small-world" networks. Nature 393:440–442.

Zhang Y, Li N, Yang J, Zhang T, Yang Z (2010) Effects of maternal food restriction on physical growth and neurobehavior in newborn Wistar rats. Brain Res Bull 83:1-8.

LEGENDS

Figure 1. Inter-group comparisons for basic network parameters: Distribution of (A) mean clustering coefficient, (B) characteristic path length and (C) small-worldness coefficient, largely overlapped between groups.

Figure 2. Between-groups correlations of connectivity weight matrices. All pairs of groups are highly associated.

Figure 3. (A) Degree frequency distribution by experimental group. Curves correspond to a Gamma distribution fitted for each group. All experimental groups displayed a very similar pattern of k distribution. (B) Rich-club index. Solid lines indicate average values and transparencies account for standard error. In the inset, the values for degrees between 15 and 18 are showed in detail. R-C indices for k larger than 14 display differences among experimental groups, with Co showing in most of the cases a larger value. (C) Schematic representation of nodes involved in rich-clubs with k>15. Nodes are represented by squares and links between them are depicted by lines. While most of the participating regions are repeated in all groups, thalamus is not present in SP.

Figure 4. PCA on ROIs volumes. Distribution along PC1 and PC2 in relation to total brain volume. Bubble size corresponds to total brain volume with the largest value being 426.22mm^3 and the smallest 333.91mm^3. On the right, a summary of some remarkable ROIs loadings for PC1 and PC2.

Figure 5. Heatmaps representing partial correlations within each experimental group.

Figure 6. (A) Total mean tract length. SP group displayed larger values compared to Co and MCP. (B) Frequency distribution of mean tract length. Curves correspond to a Gamma distribution fitted for each group. Inset: Absolute frequency of MCP and SP is subtracted to frequency of Co, the arrow indicates the drop of frequency of tracts in SP.

Table 1 Identification of studied brain regions

Number	Region name	Abbreviation
1	Olfactory bulbs right	OlfB right
2	Olfactory bulbs left	OlfB left
3	Cerebellum right	Crb right
4	Cerebellum left	Crb left
5	Corpus callosum right	CoCall right
6	Corpus callosum left	CoCall left
7	Midbrain right	Midb right
8	Midbrain left	Midb left
9	Striatum right	Str right
10	Striatum left	Str left
11	Frontal cortex right	FrCx right
12	Frontal cortex left	FrCx left
13	Temporo-parietal cortex right	TempParCx right
14	Temporo-parietal cortex left	TempParCx left
15	Hypothalamus right	Hythal right
16	Hypothalamus left	Hythal left
17	Hippocampus right	Hipp right
18	Hippocampus left	Hipp left
19	Thalamus right	Thal right
20	Thalamus left	Thal left
21	Occipital cortex right	OccCx right
22	Occipital cortex left	OccCx left
23	Fimbria left	Fim right
24	Fimbria right	Fim left

Table 2 Bartlett test for variance homogeneity

mean C	**Co**	**MCP**
Co		
MCP	5.3798 (p=0.02037)	
SP	3.0919 (p=0.07868)	0.3383 (p=0.5608)

L	**Co**	**MCP**
Co		
MCP	4.0875 (p=0.0432)	
SP	2.3414 (p=0.126)	0.2541 (p=0.6142)

Table 3 Difference between Co and SP in the mean tract length by node

Region	Difference (mm)
Cerebellum left	-0.107
Cerebellum right	-0.592
Corpus callosum left	0.132
Corpus callosum right	-0.153
Fimbria left	-0.518
Fimbria right	-0.197
Frontal cortex left	-0.073
Frontal cortex right	-0.388
Hippocampus left	-0.060
Hippocampus right	-0.437
Hypothalamus left	-0.179
Hypothalamus right	-0.003
Midbrain left	0.014
Midbrain right	-0.188
Occipital cortex left	-0.119
Occipital cortex right	-0.072
Olfactory bulb left	-0.215
Olfactory bulb right	-0.880
Striatum left	-0.310
Striatum right	-0.407
Temporo parietal cortex left	-0.515
Temporo parietal cortex right	-0.019
Thalamus left	-0.122
Thalamus right	-0.209

HIGHLIGTHS

- Maternal undernutrition impacts on the development of brain structural networks
- Connectivity parameters were differentially affected by nutritional restriction
- Rich-club structure was altered in cases of severe protein restriction
- Longer integrative tracts are less affected than shorter local ones